Synthesis of Raspberry-like PMMA/SiO_2 Nanocomposite Particles via a Surfactant-Free Method

Min Chen, Limin Wu,* Shuxue Zhou, and Bo You

Department of Materials Science, Fudan University, Shanghai 200433, P. R. China

Received July 30, 2004; Revised Manuscript Received September 29, 2004

ABSTRACT: Waterborne raspberry-like PMMA/SiO_2 nanocomposite particles were prepared via a free radical copolymerization of methyl methacrylate (MMA) with 1-vinylimidazole (1-VID) in the presence of ultrafine aqueous silica sols. The strong acid−base interaction between hydroxyl groups (acidic) of silica surfaces and amino groups (basic) of 1-VID was strong enough for promoting the formation of long-stable PMMA/SiO_2 nanocomposite particles when 10 mol % or more 1-VID as auxiliary monomer was used. The average particle sizes and the silica contents of the nanocomposite particles could range from 120 to 350 nm and 5 to 47%, respectively, depending upon reaction conditions. The influence of synthetic conditions, for instance, initial silica charge, reaction temperature, pH value, and 1-VID charge, on the particle properties was studied in detail. Stable nanocomposite particles could only be obtained at base conditions, and the silica content in the nanocomposite particles reached the maximum when pH value was 8.0. TEM and SEM indicated a raspberry-like morphology of the obtained nanocomposite particles. Zeta potential measurements confirmed that part of the 1-VID was located on the surface of the nanocomposite particles, which was consistent with the raspberry-like morphology. A possible formation mechanism of nanocomposite particles was proposed.

Introduction

In the past few years, organic−inorganic nanocomposite particles have become the subject of rapidly growing interest for their superior properties (optical, mechanical, rheological, electrical, catalytic, and fire retardance);[1−7] these nanocomposite particles usually have core−shell structures.[8−15] However, since the surfaces of inorganic particles are usually hydrophilic, while polymers are usually hydrophobic, the surfaces of inorganic particles usually need to be modified or pretreated using some so-called coupling agents in order to promote the compatibility between polymeric phase and inorganic phase to obtain core−shell morphology. For instance, Bourgeat-Lami et al.[16,17] reported the synthesis of polystyrene/silica nanocomposite particles with core−shell structure by dispersion polymerization of styrene in aqueous ethanol medium in the presence of surface-modified silica particles and poly(*N*-vinylpyrrolidone) as stabilizer. Tissot et al.[18,19] described the coating reaction of polystyrene latex with a silica layer by using a silane coupling agent to improve the compatibility of organic core and inorganic shell materials. Reculusa et al.[20] described the process of synthesizing raspberry-like core−shell hybrid particles with silica beads supporting smaller polystyrene particles via a emulsion polymerization. Fleming et al.[21] obtained raspberry-like core−shell particles by using chemical or biochemical linkages between silica microspheres and polystyrene nanospheres. Kulbaba et al.[22] took advantage of electrostatic force between positively charged polyferrocenylsilane microspheres with negatively charged silica particles to synthesize raspberry-like core−shell composite particles by self-assembly techniques. Obviously, this treatment of the surfaces of inorganic particles is very tedious and energy-consuming.

To work out this problem, Armes et al.[23−28] proposed a novel method to synthesize a series of raspberry-like core−shell nanocomposite particles with vinyl polymer as core and nanosilica as shell. In their method, 4-vinylpyridine (4-VP) was used as an auxiliary monomer. Thus, the basic property of the amino groups from 4-VP could interact with the acidic property of the hydroxyl groups from nanosilica surfaces to enhance the compatibility between organic phase and inorganic phase. This synthetic route probably has following several advantages:[24] (1) it is a simple, one-pot protocol based on readily available starting materials; (2) no surface pretreatment or modification is necessary; (3) no addition of surfactant or cosurfactant is required. However, the auxiliary monomer they involved was only 4-VP; no other auxiliary monomer was successfully tried.[23] Although they synthesized raspberry-like polymer−silica nanocomposite particles recently in the absence of any auxiliary monomers, it is limited to alcoholic medium.[29,30] Additionally, the formation mechanism of raspberry-like core−shell nanocomposite particles by this method is not clearly so far. Therefore, further work is very necessary to be done in this area.

In the present work, we first used 1-VID as the auxiliary monomer and successfully synthesized a series of long-stable raspberry-like PMMA/SiO_2 nanocomposite particles via a "soap-free" heterophase polymerization in the presence of an ultrafine aqueous silica sol and water as the continuous phase. Since the surface hydroxyl group of silica particle is acidic, the amino group (basic) of 1-VID should promote the compatibility between polymeric phase and nanosilica phase. Some influencing parameters such as initial silica charge, reaction temperature, 1-VID charge, and pH value on the nanocomposite particles were investigated in detail, and a possible formation mechanism of raspberry-like nanocomposite particles was also discussed.

Experimental Section

Materials. Methyl methacrylate (MMA) was purchased from Shanghai Chemical Reagent Co. (China) and purified by

* Corresponding author. E-mail: lxw@fudan.ac.cn.

10.1021/ma048431f CCC: $27.50
Published on Web 11/12/2004

Table 1. Typical Recipe To Synthesize Raspberry-like Nanocomposite Particles

component	amount (g)	component	amount (g)
MMA	10[a]	APS	0.1[b]
1-VID	1.66	H_2O	90
silica	18		

[a] mol (MMA):mol (1-VID) = 85:15. [b] If polymerization was performed at 40 °C, APS = 0.12 g and HSS = 0.1 g.

treating with 5% aqueous NaOH to remove the inhibitor and dried over by anhydrous calcium chloride for 3 days and then stored at low temperature prior to use. 1-Vinylimidazole (1-VID, >98%) was purchased from Yancheng Medical Chemical Co. (China) and used as received. NS-30 (20 nm silica sol, pH = 9.5) was supplied as 30 wt % aqueous dispersion by Yuda Chemical Co. (China). Ammonium persulfate (APS) was purchased from Shanghai Gaoqiao Petrochemical Co. (China) and purified by recrystallization from water. Hydrosulfite of sodium (HSS) was purchased from Shanghai Chemical Reagent Co. (China) and used as received.

Synthesis of Nanocomposite Particles. A typical synthetic process was described as follows: a known amount of 1-VID and aqueous silica sol were charged into a 250 mL round-bottom flask equipped with mechanical stirrer, thermometer with a temperature controller, an N_2 inlet, a Graham condenser, and a heating mantle and stirred at room temperature for 1 h when the pH of the solution was adjusted to the required value using 0.1 mol/L aqueous NaOH or HCl solution. The reaction mixture was then slowly added by MMA and heated to 60 °C, followed by addition of 1.0 wt % APS aqueous solution based on MMA mass. The reaction was carried at 60 °C for 24 h under a slow stream of N_2. When 1.2 wt % APS and 1.0 wt % HSS based on MMA mass were employed as the redox initiator, the reaction was performed at 40 °C for 24 h, as shown in Table 1. The resulted milky-like dispersions were purified by centrifugation−redispersion cycles for several times until no free silica particles were found by TEM. Each time successive supernatant was removed and then replaced with deionized water.

Characterization of PMMA/SiO_2 Nanocomposite Particles. *Particle Size Analysis.* Dynamic light scattering (DLS, Beckman Coulter Co.) measurements were carried out on the diluted reaction solutions to obtain the average diameters of the particles. Each sample was repeated for three times to give the average particle size.

Chemical Composition Analysis. NS-30 silica sol was dried in a vacuum oven at 60 °C for several days to obtain a constant weight and then conducted a thermogravimetric analysis using a Perkin-Elmer (TGA-7 USA) instrument to determine the loss of surface moisture. Assuming that the incombustible residues were pure silica, it was found that the loss of surface moisture is around 15 wt %. About 5 mg of dried nanocomposite particles were used to examine the SiO_2 content. All these experiments were conducted in air and heated from room temperature to 800 °C at a scan rate of 20 °C/min. The SiO_2 contents of the nanocomposite particles were calculated after subtracting the loss of surface moisture.

Morphology of Nanocomposite Particles. A transmission electron microscope (TEM Hitachi H-600, Hitachi Corp., Japan) was used to observe the morphology of obtained nanocomposite particles. The nanocomposite particles dispersions were diluted and ultrasonized at 25 °C for 10 min and then dried onto carbon-coated copper grids before examination. SEM images were obtained using scanning electron microscope (SEM Philips XL30 apparatus). The nanocomposite particles dispersions were diluted and dried on a cover glass and sputter-coated with gold prior to examination.

Zeta Potential Measurements. Zeta potential vs pH curves of original silica sol and selected PMMA/SiO_2 nanocomposite particles were constructed using a zeta potential analyzer (Zetaplus, Brookhaven Instruments Corp.). The pH of diluted nanocomposite particles dispersion was adjusted by adding either 0.1 mol/L HCl or NaOH aqueous solution.

Results and Discussion

Effect of the Initial Silica Charge. A series of nanocomposite particles were synthesized via a "soap-free" heterophase polymerization at different reaction conditions, as summarized in Table 2. The nanocomposite particles were stabilized by adsorption of hydrophilic silica particles through strong acid−base interaction between hydroxyl groups (acidic) of silica surfaces and amino groups (basic) of 1-VID, where silica particle acted as a "Pickering emulsifier".[31] Figure 1 illustrates the changes in both sizes of nanocomposite particles and SiO_2 content adsorbed on nanocomposite particles as a function of the mass ratio of SiO_2/MMA (runs 1−5 in Table 2). It was found that the average particle size ranged from 120 to 270 nm and tended to decrease with increasing initial silica charge, which had the same behavior as traditional emulsifiers. All the particles had a rather narrow size distribution, suggesting that the

Table 2. Summary of PMMA/SiO_2 Nanocomposite Particles Obtained at Different Conditions

run	MMA/1-VID mol/mol	SiO_2/MMA mass/mass	pH	T (°C)	particle size (nm) DLS	particle size (nm) TEM	conv (%)	SiO_2 (wt %)
1	85/15	1:1	9.5	60	270	180	95	15.9
2	85/15	1.4:1	9.5	60	247	165	94	16.4
3	85/15	1.8:1	9.5	60	192	120	94	17.1
4	85/15	2.2:1	9.5	60	163	100	96	18.7
5	85/15	2.6:1	9.5	60	120	85	93	20.0
6	85/15	1.4:1	9.5	40	218	150	92	22.8
7	85/15	1.4:1	9.5	60	247	165	94	17.1
8	85/15	1.4:1	9.5	70	258	180	91	15.5
9	85/15	1.4:1	9.5	80	286	185	89	12.2
10[a]	85/15	1.4:1	5.0	60				
11	85/15	1.4:1	7.5	60	301	210	92	12.1
12	85/15	1.4:1	8.0	60	186	120	91	47.0
13	85/15	1.4:1	8.5	60	213	135	91	37.7
14	85/15	1.4:1	9.0	60	246	165	95	19.2
15	85/15	1.4:1	10.0	60	318	210	93	6.1
16[b]	94/6	1:1	9.5	40				
17	90/10	1:1	9.5	40	298	200	90	15.8
18	85/15	1:1	9.5	40	264	180	89	24.6
19	80/20	1:1	9.5	40	253	175	92	25.8
20	75/25	1:1	9.5	40	245	155	93	26.9
21	70/30	1:1	9.5	40	241	150	92	25.9

[a] Polydisperse aggregates and large amounts of coagulum were obtained. [b] No stable nanocomposite particles obtained examined by TEM nanocomposite particles obtained with the other formulations kept stable for at least 6 months.

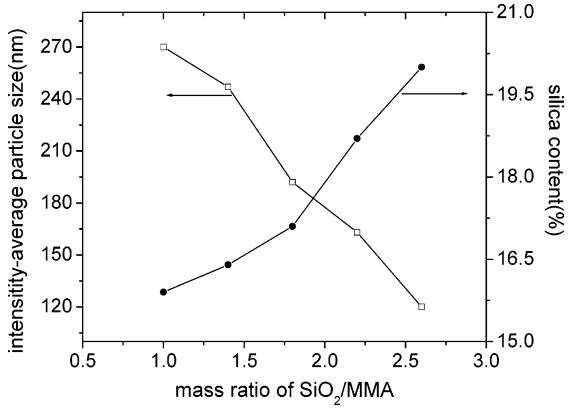

Figure 1. Dependence of particle size and silica content on the initial silica charge.

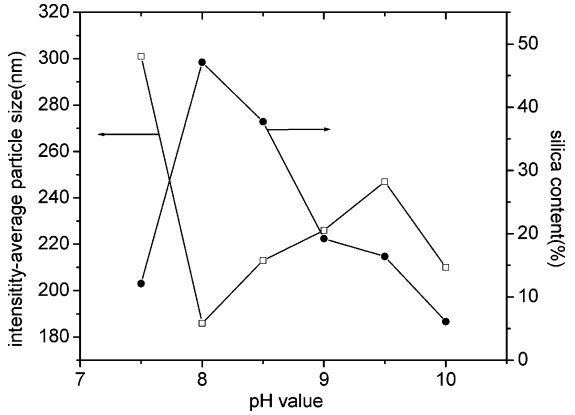

Figure 2. Effect of pH values on the particle size and silica content.

silica particles as "Pickering emulsifier" had a high stabilization power. These samples were easy to be redispersed just by shaking during the centrifugation−redispersion cycles, and TEM observed a raspberry-like morphology, in which silica beads deposited on the surfaces of organic phase. Metastable nanocomposite particles were obtained when the mass ratio of SiO_2/MMA was 0.5:1 (not listed in Table 2), and ill-shaped morphology was observed by TEM. A control experiment was carried out in the absence of any silica sol, which resulted in macroscopic precipitate and no particles formed. From these phenomena above, it seems that silica sol plays a crucial important role in the formation of nanocomposite particles and has the typical behavior as traditional emulsifiers. Armes and co-workers[26] had reported the similar rules when using 4-VP as auxiliary to prepare polymer−SiO_2 nanocomposite particles. The final silica content in the nanocomposite particles slightly increased from 15.9% to 20.0% with increasing initial silica charge, which was probably because the adsorbed silica content on the surface of organic phase nearly reached a "saturate" value when the mass ratio of SiO_2/MMA was 1:1 at this experimental pH value and reaction temperature.

Effect of Reaction Temperature. All the nanocomposite particles dispersions obtained at the studied temperatures were stable, as shown in Table 2 (runs 6−9). TEM observed a well-defined raspberry-like morphology. The data showed that the increase in reaction temperature led to slightly increase in average particle size, which was due to the higher degree of flocculation. Higher reaction temperature resulted in broader particle size distribution, further confirming more serious flocculation of the nanocomposite particles when prepared at higher temperature. However, the increase in reaction temperature decreased the silica content in the nanocomposite particles. The possible reason can be explained as follows: The auxiliary monomer, 1-VID, generally existed in three states: (1) some 1-VID was totally dissolved in the aqueous phase, (2) some was strongly adsorbed onto the silica surfaces via acid−base interaction, and (3) some was presented in the form of monomer droplets stabilized by silica particles (Pickering emulsifier). Obviously, only the latter two forms of 1-VID could contribute to adsorb silica beads during the polymerization process. The higher the reaction temperature, the more 1-VID was dissolved into aqueous phase; correspondingly, the less 1-VID participated in the adsorption process and hence decreased the silica content in the nanocomposite particles.

Effect of pH Values. Since 1-VID is a weak base and the silica surface is weakly acidic, the pH of system should have very crucial impact on the formation of nanocomposite particles. Runs 10−15 in Table 2 summarize the effect of pH values on nanocomposite particles. It turned out that only under alkaline conditions could stable nanocomposite particles be obtained. The nanocomposite particles obtained at pH = 5 showed large, polydisperse aggregates and large amounts of coagulum. There are three factors possibly influencing the pH value of the reaction systems: (1) different initial charge of the silica sol, which was served as a pH = 9.5 aqueous solution; (2) the addition of basic auxiliary monomer, 1-VID; (3) the thermal decomposition of the persulfate ions gave rise to the $[H^+]$ concentration as follows:[32] $S_2O_8^{2-} + 2H_2O \rightarrow 2OH^{\bullet} + 2SO_4^{2-} + 2H^+$. Although very complex, fortunately no pH drift was detected during the polymerization process due to the self-balance effect of the system. Therefore, the pH value was mainly controlled by adjusting using 0.1 M NaOH or HCl aqueous solution before the polymerization process started. Figure 2 more clearly demonstrated the influence of pH values of systems on the nanocomposite particles. Generally, in the basic range, the higher the pH value, the less the silica content in the nanocomposite particles; this was probably because the increase in base caused the decrease in interaction between acidic hydroxyl groups of silica surfaces and basic amino groups of 1-VID, thus decreasing the silica adsorbed onto nanocomposite particles and trying to increase particle size since much fewer silica particles acted as "Pickering emulsifier". But the reason why the nanocomposite particles obtained at pH = 7 did not obey the above general order was not clear. The silica content in the nanocomposite particles reached the maximum when pH value of the system was 8.0, suggesting that silica particles and 1-VID have the best "binding" effect at such conditions.

Effect of 1-VID Charge. The effect of 1-VID charge on the nanocomposite particles were investigated and also listed in Table 2. When 6 mol % 1-VID was added to the system, no stable nanocomposite particles obtained (see run 16 in Table 2). When 1-VID charge increased to 10 mol %, long-stable PMMA/SiO_2 nanocomposite particles were obtained. TGA indicated the silica content in the nanocomposite particles was 24.6 wt %. What is unexpected is although silica particles were deposited on the surfaces of organic particles via acid−base interaction, the silica content hardly increased with increasing the 1-VID charge from 15 to 30

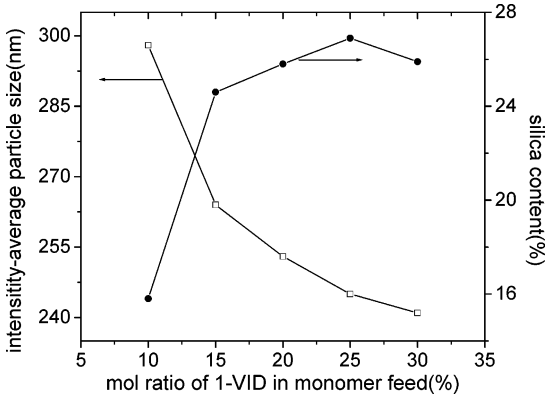

Figure 3. Effect of 1-VID content on the particle size and silica content.

mol %, as shown by runs 17−21 in Table 2 and more clearly illustrated in Figure 3; this was not coincident with the results reported by Armes et al.[24−28] when using 4-VP as auxiliary monomer. It was probably because some 1-VID did not participate in the free radical copolymerization process due to the low reactivity of 1-VID for its steric effect. To check this assumption, homopolymerization of 1-VID in the presence of silica sols was carried out at 60 °C, but no particles were found after 48 h and only some low molecular weight polymer formed. That suggested only 10 mol % 1-VID was enough to synthesize long-stable PMMA/SiO_2 nanocomposite particles with relatively high silica content.

Morphology of the Nanocomposite Particles. Figure 4 displayed some representative scanning electron micrographs of the PMMA/SiO_2 nanocomposite particles. Although the relatively low magnification did not allow us to understand the morphology of the nanocomposite particles, we still observed approximately spherical particles with uniform size. To understand whether the silica beads were deposited on the surfaces of the organic phase, the obtained nanocomposite particles were observed by high-magnification TEM. Figure 5 presented the typical TEM images of nanocomposite particles. It was found that the particle sizes were reasonably uniform and the nanocomposite particles had raspberry-like morphology with silica beads adsorbed onto the surface of the particles.

Figure 6 represented the TEM images of the PMMA/SiO_2 nanocomposite particles obtained from runs 12 and 13, which had the silica contents of 47.0% and 37.7%, respectively, as indicated in Table 2. From the images, one could see a serious flocculation of the nanocomposite particles had occurred, which should be from the strong hydrogen bonds formed between hydroxyl groups of the silica particles. This flocculation was easily cleaved under mechanical stirring, that is, typical thixotropic properties, further confirming that some hydrogen bonds formed between every two nanocomposite particles when high content silica adsorbed on nanocomposite particles.

Zeta Potential Analysis. Aqueous electrophoresis is an ideal method to analysis the surface compositions of colloidal particles, as proved by Markham[33] for poly(ethylene oxide)-stabilized polypyrrole particles and Armes[23−28,34] for polymer−silica nanocomposite particles. In the present work, zeta potential vs pH curves were obtained for original silica sol and PMMA/SiO_2 nanocomposite particles prepared by varying MMA/1-VID charge, as demonstrated in Figure 7. For original

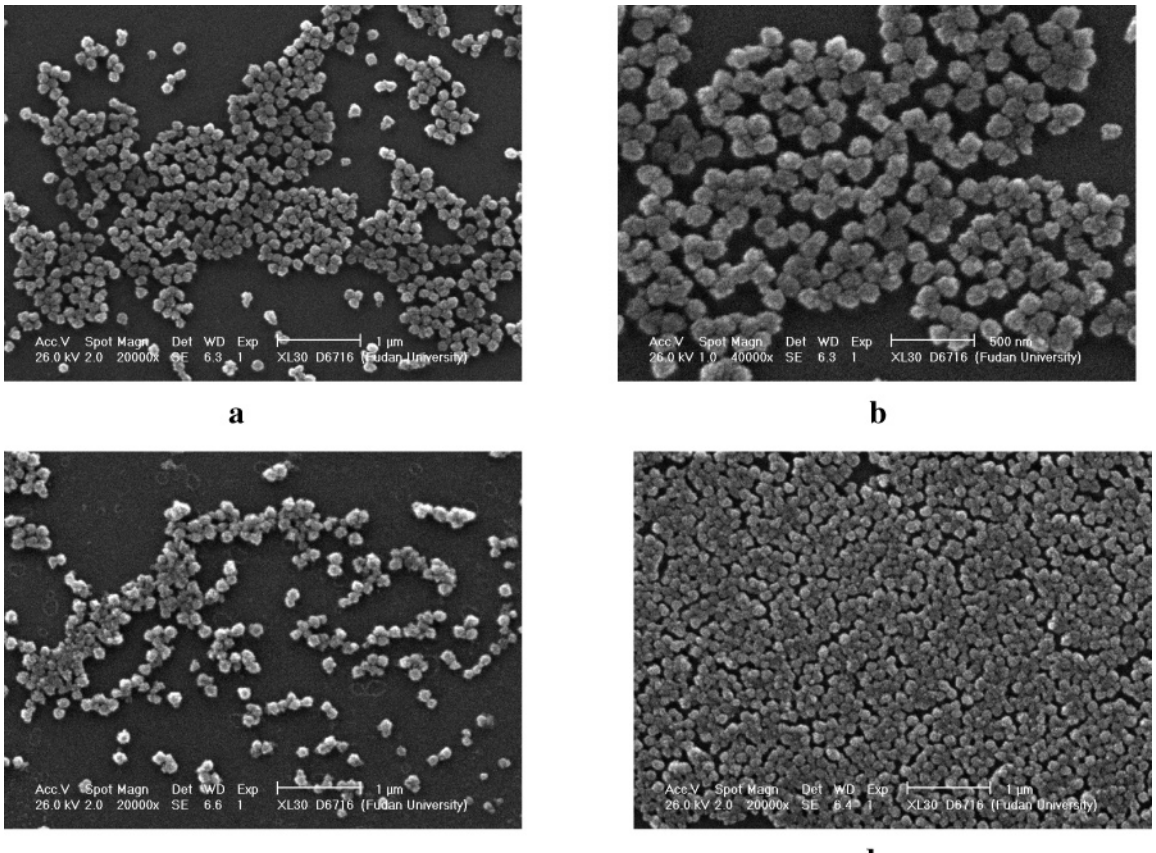

Figure 4. Representative SEM images of obtained nanocomposite particles: a, run 2; b, run 7; c, run 12; d, run 19.

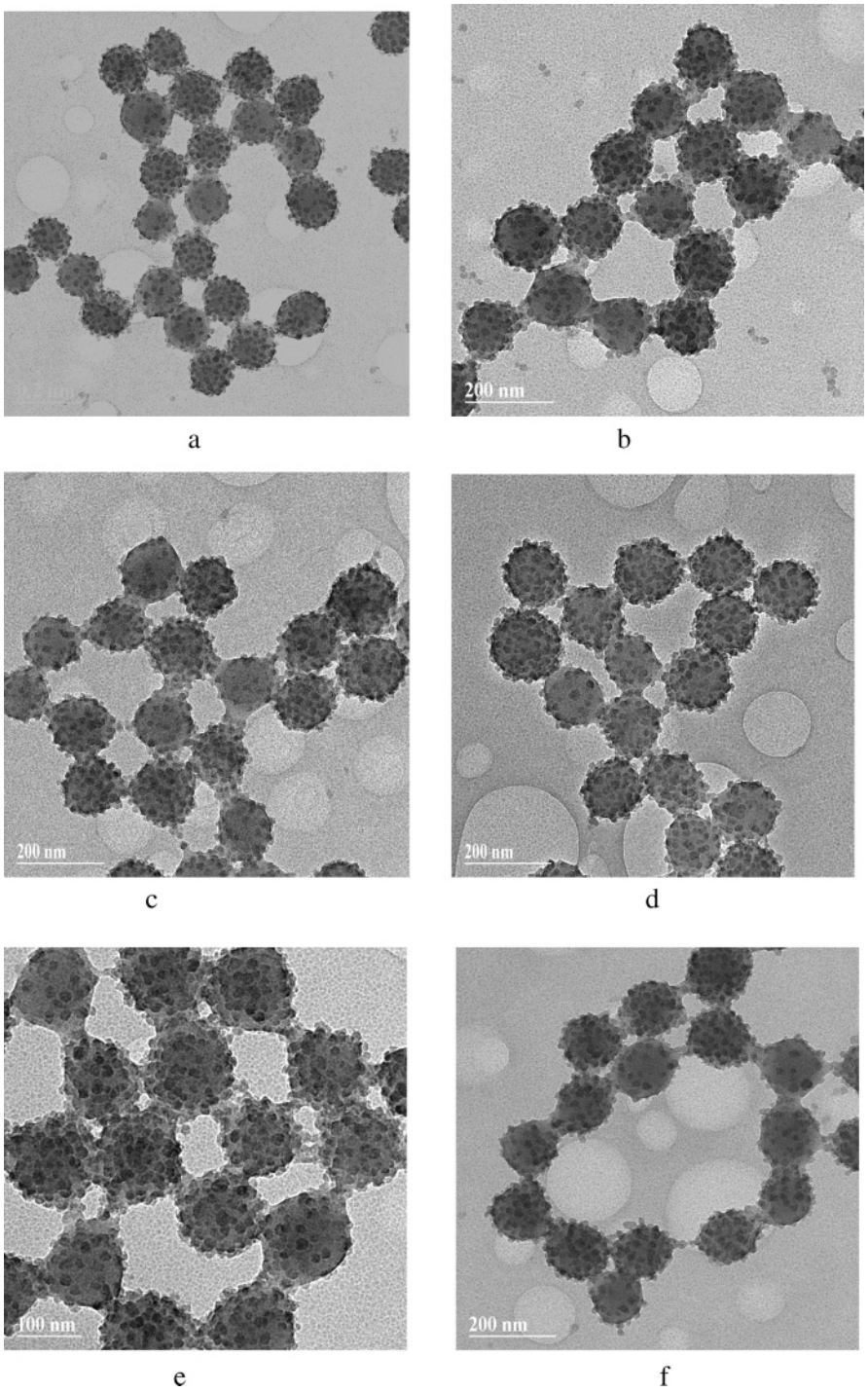

Figure 5. TEM images of obtained nanocomposite particles (a, b: run 3; c, d: run 9; e, f: run 19).

silica sol, negative zeta potential was observed over the whole pH range examined. In contrast, the zeta potential vs pH curves for the PMMA/SiO_2 nanocomposite particles showed the existence of isoelectric point at approximately pH = 6 and positive zeta potential of up to +50 mV was obtained at low pH. Thus, this observation provided good evidence that the basic 1-VID were partly located at the surfaces of the nanocomposite particles and strongly influenced the zeta potential. At low pH, they were protonated and hence cationic, which resulted in the positive zeta potential. However, increasing the initial 1-VID charge led to high positive zeta potential at low pH, which was due to the increased surface concentration of 1-VID in the nanocomposite particles. Maybe this observation can further interpret how the raspberry-like PMMA/SiO_2 nanocomposite particles formed.

Formation Mechanism of PMMA/SiO_2 Nanocomposite Particles. To understand the formation mechanism of PMMA/SiO_2 nanocomposite particles, a control experiment without any silica sol was carried out, which only resulted in macroscopic precipitate and no particles formed. In the meantime, another experiment was carried out in the absence of any 1-VID, as illustrated in Figure 8a, the resulted milky-like dispersion was metastable and became coagulum after a few days. TEM images of the metastable particles indicated some bare PMMA particles and free silica beads existed. TGA showed only 3% silica content was adsorbed onto the particle surface due to the hydrogen bonding between

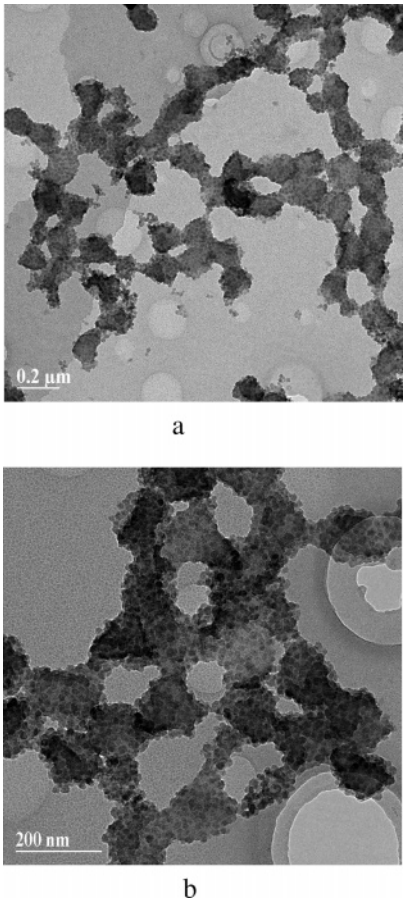

Figure 6. TEM images of obtained nanocomposite particles with high silica content: a, run12; b, run 13.

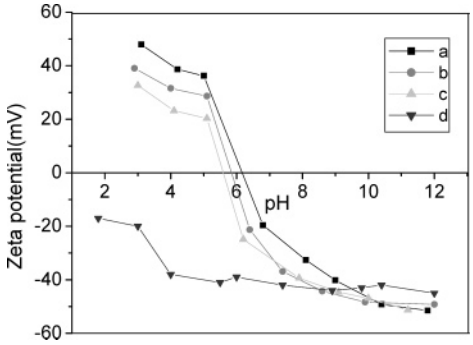

Figure 7. Zeta potential vs pH curves for nanocomposite particles prepared by varying MMA/1-VID mol ratio (a−c) and original silica sol (d). (a) MMA/1-VID = 70:30, (b) MMA/1-VID = 80:20, (c) MMA/1-VID = 90:10, (d) original silica sol.

silanol functions with carbonyl group of the PMMA. However, if 1-VID was introduced to the reaction system, a raspberry-like PMMA/SiO_2 nanocomposite particle was obtained. Figure 8b showed the reaction scheme for the formation of PMMA/SiO_2 nanocomposite particles. Combined with the results of zeta potential measurements, it seemed that 1-VID acted as a "binder" to connect the organic phase with inorganic silica particles. Since our nanocomposite particles were obtained in aqueous media without any surfactants or polymeric stabilizers, the hydrophilic ultrafine silica beads herein acted as emulsifier to stabilize the nanocomposite particles. In the present work, the solubility of the organic phase is neglectable in aqueous media; we suggested that the raspberry-like particle morphology was obtained directly from the polymerization of

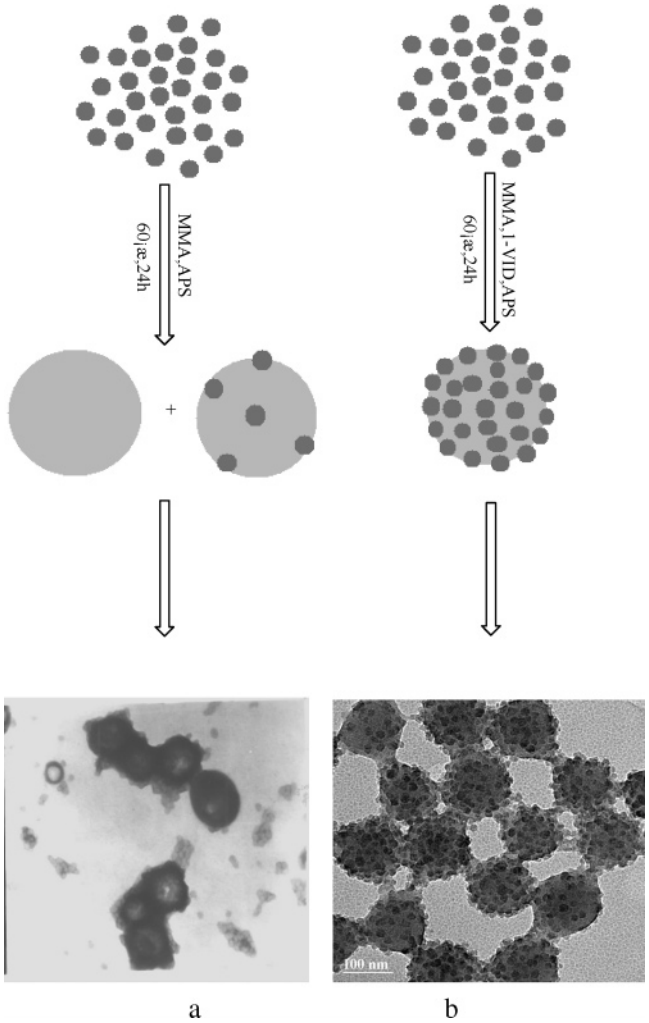

Figure 8. Reaction scheme for the formation of PMMA/SiO_2 nanocomposite particles.

silica-stabilized monomer droplets. If this mechanism were true, some oil-soluble initiators dissolved in monomer would lead to a "bulk" polymerization in the monomer droplets, which also caused raspberry-like organic/inorganic nanocomposite particles. If so, the polymerization locus and the formation mechanism of nanocomposite particles should be better understood; a related investigation is underway. By using this "soap-free" heterophase polymerization method, some other nano-inorganic particles, for instance, Fe_3O_4, Al_2O_3, TiO_2 and so on, are of great potential to synthesize versatile organic/inorganic nanocomposite particles.

Conclusions

A series of raspberry-like PMMA/SiO_2 nanocomposite particles were successfully synthesized in the presence of ultrafine silica aqueous sols with 1-VID as auxiliary monomer via a "soap-free" heterophase polymerization process. These particles had a reasonably narrow size distribution, and average particle sizes were in the range of 120−350 nm and silica contents were up to 47% by varying the initial silica charge, reaction temperature, pH value of the system, and 1-VID charge. TEM combined with zeta potential measurement confirmed the raspberry-like morphology of the obtained PMMA/SiO_2 nanocomposite particles. On the basis of this study, we would believe that the raspberry-like particle

morphology was obtained directly from the polymerization of silica-stabilized monomer droplets.

Since adjusting the glass transition temperature of organic phase could control the film-forming property of nanocomposite particles and the reaction media was aqueous, these composite particles are of great potential interest as environmentally friendly tough, abrasion-resistant, transparent coatings.

Acknowledgment. We thank the National "863" Foundation, Shanghai Nano Special Foundation, the Key Project of China Educational Ministry, the Doctoral Foundation of University, and Trans-century Outstanding Talented Person Foundation of China Educational Ministry for financial support of this research.

References and Notes

(1) Sanchez, C.; Soler-Illia, G. J. de A. A.; Ribot, F.; Lalot, T.; Mayer, C. R.; Cabuil, V. *Chem. Mater.* **2001**, *13*, 3061.
(2) Caruso, F. *Adv. Mater.* **2001**, *13*, 11.
(3) Caruso, F.; Spasova, M.; Susha, A.; Giersig, M.; Caruso, R. A. *Chem. Mater.* **2001**, *13*, 109.
(4) Beecroft, L. L.; Ober, C. K. *Chem. Mater.* **1997**, *9*, 1302.
(5) Zhu, J.; Morgan, A. B.; Lamelas, F. J.; Wilkie, C. A. *Chem. Mater.* **2001**, *13*, 3774.
(6) Manias, E.; Touny, A.; Wu, L.; Strawhecker, K.; Lu, B.; Chung, T. C. *Chem. Mater.* **2001**, *13*, 3516.
(7) Hu, Y. Q.; Wu, H. P.; Gonsalves, K. E.; Merhari, L. *Microelectron. Eng.* **2001**, *56*, 289.
(8) Xia, Y.; Gates, B.; Yin, Y.; Lu, Y. *Adv. Mater.* **2000**, *12*, 693.
(9) Antellmi, D. A.; Spalla, O. *Langmiur* **1999**, *15*, 7478.
(10) Zhong, Z.; Yin, Y.; Gates, B.; Xia, Y. *Adv. Mater.* **2000**, *12*, 206.
(11) Zhang, M.; Gao, G.; Li, C.; Liu, F. *Langmuir* **2004**, *20*, 1420.
(12) Erdem, B.; Sudol, E. D.; Dimonie, V. L.; El-Aasser, M. S. *J. Polym. Sci., Polym. Chem.* **2000**, *38*, 4431.
(13) Landfeste, K.; Tiarks, F.; Hentze, H.; Antonietti, M. *Macromol. Chem. Phys.* **2000**, *201*, 1.
(14) Quaroni, L.; Chumanov, G. *J. Am. Chem. Soc.* **1999**, *121*, 10642.
(15) Landfeste, K. *Adv. Mater.* **2001**, *13*, 765.
(16) Bourgeat-Lami, E.; Lang, J. *Colloid Interface Sci.* **1998**, *197*, 293.
(17) Luna-Xavier, J. L.; Bourgeat-Lami, E.; Guyot, A. *Colloid Polym. Sci.* **2001**, *279*, 947.
(18) Tissot, I.; Novat, C.; Lefebvre, F.; Bourgeat-Lami, E. *Macromolecules* **2001**, *34*, 5737.
(19) Tissot, I.; Reymond, J. P.; Lefebvre, F.; Bourgeat-Lami, E. *Chem. Mater.* **2002**, *14*, 1325.
(20) Reculusa, S.; Poncet-Legrand, C.; Ravaine, S.; Mingotaud, C.; Duguet, E.; Bourgeat-Lami, E. *Chem. Mater.* **2002**, *14*, 2354.
(21) Fleming, M. S.; Mandal, T. K.; Walt, D. R. *Chem. Mater.* **2001**, *13*, 2210.
(22) Kulbaba, K.; Resendes, R.; Cheng, A.; Bartole, A.; Safa-Senat, A.; Coombs, N.; Stöver, H. D. H.; Greedan, J. E.; Ozin, G. A.; Manners, I. *Adv. Mater.* **2001**, *13*, 732.
(23) Barthet, C.; Hickey, A. J.; Cairns, D. B.; Armes, S. P. *Adv. Mater.* **1999**, *11*, 408.
(24) Percy, M. J.; Michailidou, V.; Armes, S. P. *Langmiur* **2003**, *19*, 2072.
(25) Agarwal, G. K.; Titman, J. J.; Percy, M. J.; Armes, S. P. *J. Phys. Chem. B* **2003**, *107*, 12497.
(26) Amalvy, J. I.; Percy, M. J.; Armes, S. P. *Langmiur* **2001**, *17*, 4770.
(27) Han, M. G.; Armes, S. P. *Langmiur* **2003**, *19*, 4523.
(28) Percy, M. J.; Barthet, C.; Lobb, J. C.; Khan, M. A.; Lascelles, S. F.; Vamvakaki, M.; Armes, S. P. *Langmiur* **2000**, *16*, 6913.
(29) Percy, M. J.; Amalvy, J. I.; Randall, D. P.; Armes, S. P. *Langmiur* **2004**, *20*, 2184.
(30) Percy, M. J.; Armes, S. P. *Langmiur* **2002**, *18*, 4562.
(31) Vignati, E.; Piazza, R. *Langmiur* **2003**, *19*, 6650.
(32) Bartlett, P. D.; Nozaki, K. *J. Polym. Sci.* **1948**, *3*, 216.
(33) Butterworth, M. D.; Corradi, R.; Johal, J.; Lascelles, S. F.; Maeda, S.; Armes, S. P. *J. Colloid Interface Sci.* **1995**, *174*, 510.
(34) Amalvy, J. I.; Unali, G.-F.; Li, Y.; Granger-Bevan, S.; Armes, S. P. *Langmiur* **2004**, *20*, 4345.

MA048431F